LiPB Dynamic Cell Models for Kalman-Filter SOC Estimation

Gregory L. Plett

Abstract

This paper reports some results relating to dynamic cell modeling for the underlying purpose of state-of-charge (SOC) estimation in a hybrid-electric-vehicle (HEV) application. The cells in question are Lithium Ion Polymer based, jointly developed by LG Chem Ltd. (Daejeon, Korea) and Compact Power Inc. (Colorado, USA), have a nominal capacity of about 8Ah, and are optimized for power-needy applications.

The HEV application is a very harsh environment, with rate requirements up to about ±25C and very dynamic rate profiles. This is in contrast to relatively benign portable-electronic applications with constant power output and fractional C rates. Methods for estimating SOC that work well in portable-electronic devices may not work well in the HEV application. If precise SOC estimation is required by the HEV, then a very accurate cell model is necessary.

The SOC estimation method we use is based on a Kalman-filtering method, and is described in a companion paper to be presented at this conference [1]. A requirement that this approach imposes on the cell model is that SOC be a state in the model state vector.

Several different cell models are presented. The simplest one uses "Coulomb counting" as the state equation, and Shepherd's rule as the output equation. This model does not predict relaxation dynamics of the cell. An enhanced model adds filter states to take into account relaxation and other dynamics in closed-circuit cell voltage, and works better. A method based on nonlinear autoregressive filtering and dynamic radial basis function networks produces the best results overall.

Results of lab tests on physical cells, compared with model prediction, are presented. The best results obtained to date model the cell so precisely that the RMS estimation error is less than the quantization noise floor expected in our battery-management-system design. More importantly, the model allows very precise SOC estimation, therefore allowing the vehicle controller to confidently use the battery pack's full operating range without fear of over- or under-charging cells. *Copyright*$^{©}$ *2002 EVS19*

Keywords: Modeling, battery model, battery management, lithium polymer, state of charge.

1. Introduction

This paper describes some methods to model the electrical input-output behavior of Lithium Ion Polymer Battery (LiPB) cells. The cells are treated as nonlinear dynamic systems, represented in a discrete-time state-space form. Specifically, we assume the form

$$x_{k+1} = f(x_k, u_k) + w_k \tag{1}$$
$$y_k = g(x_k, u_k) + v_k, \tag{2}$$

where x_k is the system state vector at discrete-time index k, u_k is the measured exogenous system input at time k (which may include measurements of battery-pack current, temperature and so forth) and w_k is unmeasured "process noise" affecting the system state (and also models the inaccuracy of the cell

model, to some extent). The system output is y_k and v_k is the measurement noise that usually models noise in sensors. In the equations, $f(\;)$ and $g(\;)$ are (possibly nonlinear) functions, specified by the particular cell model used.

To be more specific, the system input vector u_k typically contains the instantaneous cell current i_k. It may also contain the cell temperature T_k, an estimate of the cell's capacity C, and/or an estimate of the cell's internal resistance R_k, for example. The system output is typically a scalar but may be vector valued as well. Here we consider the output to be the cell's loaded terminal voltage (not at-rest OCV). The system's state vector x_k in some way represents in summary form the total effect of all past input to the system so that the present output may be predicted solely as a function of the state and present input. Values of past inputs are not required. Our method constrains the state vector to include SOC as one component, as described in Section 3.

Many cell models have been proposed in the literature for many purposes. Section 2 outlines a few of these. The specific application we have in mind is to model cell dynamics for the purpose of state-of-charge estimation in a hybrid electric vehicle (HEV) battery pack. The HEV application is a very harsh environment with rate requirements up to about ±25C, very dynamic rate profiles, and operating temperatures between –30ºC and 50ºC. This is in contrast to relatively benign portable-electronic applications with constant power output and fractional C rates. Methods for cell modeling and SOC estimation that work well in portable electronic devices often fail in the HEV application. If precise SOC estimation is required by the HEV, then a very accurate cell model is necessary.

The cells modeled in this paper are Lithium-Ion Polymer based, jointly developed by LG Chem, Ltd. (Daejeon, Korea) and Compact Power Inc. (Colorado, USA), have a nominal capacity of about 8 Ah, and are optimized for power-needy applications. The approach presented in this paper very accurately models the dynamics of these cells. The method is also very general, and we expect it to work well in many other battery systems with different chemistries and applications.

This paper is organized as follows: First, a brief literature review of SOC estimation methods with companion cell modeling approaches is given. Secondly, we explain how our approach differs with the simple requirement that SOC be an element of the system state, and the advantages that accrue from this choice. Thirdly, some candidate cell model structures are proposed, along with methods for determining model parameters. The testing equipment, cells and regimen for cell modeling are described. Finally, the results are evaluated and conclusions made.

2. Some Alternate Methods for Cell Modeling and SOC Estimation

We proceed by examining the literature to see if present methods meet our needs. Recall that our application is to model cell dynamics for the purpose of SOC estimation in an HEV battery pack. We find that many papers on cell modeling do not directly consider estimating SOC, and that many papers on estimating SOC include some description of cell modeling. Therefore, many of the references cited are SOC estimation papers. An excellent summary of all of these methods, in greater detail than can be presented here, may be found in reference [2].

For the application in mind, the cell model must be accurate for all operating conditions. These include: very high rates (many papers consider rates up to about ±1C for portable electronic applications; we need to consider rates up to about ±25C), temperature variation in the automotive

range of –30ºC to 50ºC, very dynamic rates (unlike the more benign portable electronic and battery electric vehicle application). Charging (regen) must be accounted for in the method.

We also require non-invasive methods using only readily available signals. This requirement is imposed by the HEV environment where the battery management system (BMS) has no direct control over current and voltage experienced by the battery pack—this is in the domain of the vehicle controller and inverter. This requirement implies that we must rely on such measurements as instantaneous cell terminal voltage, cell current and cell external temperature.

Our cell chemistry also limits the range of approaches we might consider. Techniques specific to lead-acid chemistries, for example, are not appropriate for LiPB cells.

2.1. Laboratory and Chemistry-Dependent Methods

Several methods simply cannot be used in our application. (1) A laboratory method for determining SOC is to completely discharge a cell to determine its present remaining capacity. This is impossible and counter-productive in the HEV application. (2) Chemistry-dependent methods for lead-acid batteries, such as *Coup de Fouet* measurement, or measurement of electrolyte physical properties, are all inappropriate (as our application uses LiPB cells). (3) Open-circuit voltage measurements: If the cell is allowed to rest for a long period, its terminal voltage decays to OCV, and OCV may be used to infer SOC (via a lookup table, for example). However, long periods (sometimes hours) of battery inactivity must occur before the terminal voltage approaches OCV. This method is impractical for dynamic SOC estimation.

2.2. Electro-chemical Modeling

One approach to modeling cell electrical dynamics is to very carefully consider, at the chemical reaction level, the various processes that occur within the cell. Some inputs to this modeling process include knowledge of the reaction occurring at the anode and cathode, and understanding of the electrolyte ion transfer process. Very accurate terminal voltage prediction may be achieved by these models (see reference [3], for example). However, there is no evident way to extract SOC from the model, and it would be difficult (if possible) to measure the many required physical parameters on a cell-by-cell basis in a high-volume consumer product. We have not pursued this approach.

2.3. Impedance Spectroscopy

Another broad category of cell modeling involves measuring cell impedances over a wide range of a.c. frequencies [4–8]. Typically, an equivalent circuit model is made of the cell using resistors, capacitors, inductors, and/or complex impedances. Values of the model parameters are found by least squares fitting to measured impedance values. SOC is generally an input to the model as cell impedance is a function of SOC. Therefore, SOC may be indirectly inferred by measuring cell impedance and correlating them with known impedances at various SOC levels.

We must also discount this method for our application, as we have no direct method to inject signals into cells to measure impedances. We rely on the vehicle to generate and dissipate all energy flowing through the battery pack. The impedances might be generated using a fast Fourier transform (FFT) approach and available measurements as $Z(e^{j\omega})=E(e^{j\omega})/I(e^{j\omega})$, but again we would need to guarantee that $i(t)$ was "persistently exciting" and that $I(e^{j\omega})$ had no zero values. This guarantee would be violated, for example, if the battery pack were at rest for some period, which is a frequent event.

Depending on the block length of the FFT, the method could also impose an unacceptable time delay in measuring impedance and hence SOC.

2.4. Circuit Models

A number of papers present equivalent circuit models of cells [9–12]. Typically, a high-valued capacitor is used to represent the open-circuit voltage (OCV). The remainder of the circuit models the cell's internal resistance and more dynamic effects such as terminal voltage relaxation. From the OCV estimate, SOC may be inferred via table lookup.

Both linear- and nonlinear-circuit models may be used. We have found that linear circuit models do not work as well as we would like.

2.5. Coulomb Counting

The final method discussed in the literature involves SOC estimation directly via Coulomb counting. This may be done "open-loop", which is often very imprecise due to sensor error, or "closed loop" which is more accurate. The feedback mechanism may be empirically designed [13] or use a more theoretically justified approach such as a Kalman Filtering method [14–15] to generate the feedback. All Kalman-filtering based methods in the literature (with which we are familiar) use a circuit model of the cell with capacitor voltages representing OCV and relaxation effects. OCV may be estimated and SOC inferred from OCV.

Our approach is also based on the Kalman filtering method, but the fundamental aspect of our model that sets it apart from those reported in the literature is that SOC is directly a state of the system. The large benefit of this approach is that the Kalman filter directly gives a dynamic estimate of the SOC and its uncertainty (this is discussed in greater detail in the companion paper [1]). That is, instead of reporting the SOC to the vehicle controller (at some point in time) to be "about 55%", the algorithm is able to report that the SOC is 55%±7%, for example. This allows the vehicle controller to confidently use the battery pack's full operating range without fear of over- or under-charging cells.

3. Model Structures

In order to use the Kalman methods we propose to estimate SOC, the cell model must be represented in discrete-time state-space form. Specifically, we assume the form of equations (1) and (2). The difference between the models, then, depends on the definitions of x_k, u_k, $f(\ )$ and $g(\ )$.

We also require that SOC is a member of the state vector. To be complete, we give a list of definitions culminating in a careful definition of SOC.

Definition: The cell high operational voltage limit is called v_h. Here, we may use v_h=4.2V.
Definition: The cell low operational voltage limit is called v_l. Here, we may use v_l=3.0V.
Definition: A cell is *fully charged* when its voltage reaches $v=v_h$ after being charged at infinitesimal current levels.
Definition: A cell is *fully discharged* when its voltage reaches $v=v_l$ after being drained at infinitesimal current levels.
Definition: The *capacity* of a cell is the maximum number of Ampere-hours that can be drawn from the cell before it is fully discharged, at room temperature (25°C), starting with the cell fully charged.

Definition: The *nominal capacity* of the cell is the number of Ampere-hours that can be drawn from the cell at room temperature at the C/40 rate, starting with the cell fully charged.

Definition: The SOC of the cell is the ratio of the remaining capacity to the nominal capacity of the cell, where the remaining capacity is the number of amp-hours that can be drawn from the cell at room temperature at the C/40 rate.

With these definitions in place, we can then investigate some mathematical relations involving SOC. Particularly,

$$SOC(t) = SOC(0) - \int_0^t \frac{\eta(i(\tau))i(\tau)}{C} d\tau, \tag{3}$$

where C is the nominal capacity of the cell, $i(t)$ is the cell current at time t, and $\eta(i(t))$ is the Coulombic efficiency of the cell. (Here, we use $\eta(i(t))=1$ for discharge and $\eta(i(t))=0.995$ for charge). A discrete-time approximate recurrence may then be written as

$$SOC_{k+1} = SOC_k - \frac{\eta(i_k)i_k \, \Delta t}{C}, \tag{4}$$

where Δt is the sampling period (in hours). Equation (4) is the basis for including SOC in the state vector of the cell model as it is in state equation format already, with SOC as the state and i_k as the input. Our cell models will then be differentiated by the additional components in the state vector and the functional form of $f(\ )$ and $g(\ )$.

3.1. Models with a Single State

We will first investigate models with a single state; *i.e.,* SOC. These models share a common process equation (4). The difference between them is then the output equation. Several different forms are suggested in reference [16].

Shepherd model:	$y_k = 4.2 - R\,i_k - K_i / SOC_k$	(5)
Unnewehr universal model:	$y_k = 4.2 - R\,i_k - K_i\,SOC_k$	(6)
Nernst model:	$y_k = 4.2 - R\,i_k + K_1 \ln(SOC_k)$	(7)
Modified Nernst model:	$y_k = 4.2 - R\,i_k + K_2 \ln(SOC_k) + K_3 \ln(1-SOC_k)$	(8)

In these models, y_k is the cell terminal voltage, R is the cell internal resistance (different values may be used for charge/discharge and at different SOC levels if desired), K_i is the polarization resistance and K_1, K_2, and K_3 are constants chosen to make the model fit the data well. The "modified Nernst" model of (8) reflects an additional term that we added to the Nernst model to cause it to fit our data better. All of the terms of (5) through (8) may be collected to make a "combined model" that performs better than any of the individual models alone.

Combined model: $\quad y_k = K_0 - R\,i_k - K_1/SOC_k - K_2\,SOC_k + K_3 \ln(SOC_k) + K_4 \ln(1-SOC_k)$ (9)

The unknown quantities in (9) may are estimated using a system identification procedure. This model has the advantage of being "linear in the parameters"; that is, the unknowns occur linearly in the output equation. A simple way to find the parameters is then as follows: We first form the vector $Y = [y_1, y_2, \ldots y_N]^T$ and the matrix $H = [h_1^T, h_2^T, \ldots h_N^T]^T$. The rows of H are (transposes of) $h_j = [1, i_j^+, i_j^-, 1/SOC_j, SOC_j, \ln(SOC_j), \ln(1-SOC_j)]^T$, where i_j^+ is equal to i_j if $i_j > 0$, i_j^- is equal to i_j if $i_j < 0$, else i_j^+ and i_j^- are zero. Then,

$$Y = H\theta,$$

where $\theta = [K_0, R^+, R^-, K_1, K_2, K_3, K_4]^T$ is the vector of unknown parameters. The least-squares solution for θ is

$$\theta = (H^T H)^{-1} H^T Y.$$

This may be evaluated in Matlab, for example, as `theta=H\Y;`

3.2. Models with Multiple States to Track Relaxation

The combined model of (9) may be very quickly identified and implemented. Its serious limitation is that it omits any description of cell relaxation. Since the cell model must accurately predict its behavior in a dynamic HEV environment, we find it is essential to include relaxation effects.

In a state-variable model, dynamics are described by the state equation (1). Therefore, to include relaxation effects, we must augment the state vector with additional filter states. We choose to implement filtered versions of SOC and the input current. The resulting model is then:

$$x_{k+1} = \begin{bmatrix} 1 & 0 & 0 & 0 \\ w_1 & w_2 & 0 & 0 \\ 0 & 0 & w_4 & w_5 \\ 0 & 0 & -w_5 & w_4 \end{bmatrix} x_k + \begin{bmatrix} -1 & 0 \\ 0 & 1 \\ 0 & 0 \\ 1 & 0 \end{bmatrix} \begin{bmatrix} I_k^{\text{mod}} \\ w_3 \end{bmatrix}$$

$$y_k = w_6 + w_7 I_k^{\text{mod}} + \frac{w_8}{x_{k,1} + w_9} + \begin{bmatrix} w_{10} & 10 & w_{11} & w_{12} \end{bmatrix} x_k,$$

where $I_k^{\text{mod}} = \eta(i_k) |i_k|^n \Delta t / C_p$, n is the Peukert exponent and C_p is the Peukert capacity. The first state of x_k (that is, $x_{k,1}$) is SOC, as before. The output y_k is terminal voltage, as before. The parameters of the model are found by system identification using measured cell data. We found that the model was able to predict cell behavior best when different sets of parameters were used for different levels of input current i_k.

We will use a Kalman filter to estimate the state of a dynamic system; *e.g.,* to estimate the cell SOC.[1] We may also use a Kalman filter to perform system identification. To do so, consider the weights (parameters) of the cell model to be the state of some "true" dynamic system:

$$W_{k+1} = W_k$$

$$d_k = y_k + v_k.$$

Here, W_k is the "truth/optimum" weight vector at time k and has as components the weights w_1 through w_{12}. The optimum weight vector is constant, explaining the dynamics in the top line. The "output" of the optimum weight dynamics is the desired response, which is equal to the cell output plus the estimation error. We can create an extended Kalman filter to iteratively estimate the state (weight vector) of the cell model:

$$\hat{W}_{k+1} = \hat{W}_k + L_k (d_k - y_k)$$

$$L_k = P_k C_k \left[C_k^T P_k C_k + R_k \right]^{-1}$$

$$P_{k+1} = P_k - L_k C_k^T P_k.$$

Here, P_k is the approximate conditional error covariance matrix, initialized to a diagonal matrix with small values, $R_k \leq 1$, and $C_k^T = dy_k / dW$.

---

[1] This is covered in detail in reference [1]. The system identification procedure may also be best understood by consulting this reference for details on Kalman filtering. See also reference [17].

To compute dy_k / dW we first note that $y_k = fn(x_k, I_k^{\text{mod}}, W)$, $x_k = fn(x_{k-1}, I_{k-1}^{\text{mod}}, W)$ and use the chain rule for total differentials.

$$\frac{dx_k}{dW} = \frac{\partial x_k}{\partial W} + \underbrace{\frac{\partial x_k}{\partial x_{k-1}}}_{A_{k-1}} \frac{dx_{k-1}}{dW} + \frac{\partial x_k}{\partial I_{k-1}^{\text{mod}}} \underbrace{\frac{dI_{k-1}^{\text{mod}}}{dW}}_{0}$$

$$\frac{dy_k}{dW} = \frac{\partial y_k}{\partial W} + \frac{\partial y_k}{\partial x_k} \frac{dx_k}{dW} + \frac{\partial y_k}{\partial I_{k-1}^{\text{mod}}} \underbrace{\frac{dI_{k-1}^{\text{mod}}}{dW}}_{0}$$

In the second line,

$$\frac{\partial y_k}{\partial W} = \begin{bmatrix} 0 & 0 & 0 & 0 & 0 & 1 & I_k^{\text{mod}} & \dfrac{1}{x_{k,1} + w_9} & \dfrac{-w_8}{(x_{k,1} + w_9)^2} & x_{k,1} & x_{k,3} & x_{k,4} \end{bmatrix},$$

$$\frac{\partial y_k}{\partial x_k} = \begin{bmatrix} w_{10} & 10 & w_{11} & w_{12} \end{bmatrix} + \begin{bmatrix} \dfrac{-w_8}{(x_{k,1} + w_9)^2} & 0 & 0 & 0 \end{bmatrix} = \begin{bmatrix} w_{10} - \dfrac{w_8}{(x_{k,1} + w_9)^2} & 10 & w_{11} & w_{12} \end{bmatrix},$$

and dx_k / dW is computed in the first line.

In the first line,

$$\frac{\partial x_k}{\partial W} = \begin{bmatrix} 0 & 0 & 0 & 0 & 0 & 0 & 0 & 0 & 0 & 0 & 0 \\ x_{k-1,1} & x_{k-1,2} & 1 & 0 & 0 & 0 & 0 & 0 & 0 & 0 & 0 & 0 \\ 0 & 0 & 0 & x_{k-1,3} & x_{k-1,4} & 0 & 0 & 0 & 0 & 0 & 0 & 0 \\ 0 & 0 & 0 & x_{k-1,4} & -x_{k-1,3} & 0 & 0 & 0 & 0 & 0 & 0 & 0 \end{bmatrix},$$

$$\frac{\partial x_k}{\partial x_{k-1}} = A_{k-1} = \begin{bmatrix} 1 & 0 & 0 & 0 \\ w_1 & w_2 & 0 & 0 \\ 0 & 0 & w_4 & w_5 \\ 0 & 0 & -w_5 & w_4 \end{bmatrix},$$

and dx_{k-1} / dW is a previously computed and stored version of dx_k / dW. All terms are accounted for, and the algorithm is complete.

3.3. Radial Basis Function Model

Adding linear filter states to the model does improve its ability to predict a cell's behavior. However, as the LiPB cells themselves are nonlinear systems, we can improve even further by considering a fully nonlinear dynamic cell model. For this purpose, we will use radial-basis-function (RBF) networks and a black-box system identification procedure.

An RBF network makes a local approximation of the function it models. It computes its output as a weighted sum of (hyper) Gaussian shapes. Specifically, it computes the function

$$y_k = \sum_{j=1}^{N} w_j \exp\left(-\frac{1}{\sigma_j^2} \|u_k - t_j\|^2 \right) + w_{N+1},$$

where N is the number of bases, w_j is the weight connecting the jth basis function to the output, σ_j is the "standard deviation" or width parameter of the jth basis function, x_k is the vector input to the network, and t_j is the center of the jth basis function. Here, u_k includes the states of the system: e.g., $x_k = [y_{k-1}, \text{SOC}_k]^T$ as well as the cell current i_k.

A cartoon illustrating how RBFs approximate some smooth function is drawn in Fig. 1. The red line is the function to be approximated. The two blue Gaussian shapes with different centers, widths and heights sum together to closely approximate the red line. The same idea applies in higher dimensions. When training an RBF, the goal is to find the correct set of centers, widths and output scales to approximate the function of interest.
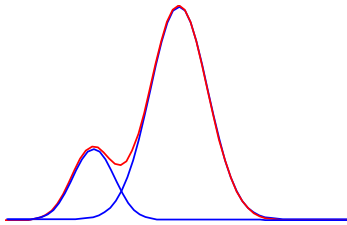

Figure 1: Cartoon illustrating how the function drawn as a red line may be approximated by the sum of two Gaussian shapes drawn as blue lines.

The parameters of a RBF network may be identified from data using a Kalman filter in the same way as described in Section 3.2. The details will not be discussed here.

4. Cell Testing and Model Fitting Results

In order to compare the abilities of the proposed models to capture a cell's dynamics, we gathered data from some prototype LiPB cells. We used a Tenny thermal chamber set at 25°C and an Arbin cell cycler. In all cases, the cells were fully charged before the tests began. Pulsed discharge cycles punctuated with rest intervals were followed by pulsed charge cycles, again with rest periods. Data points (including voltage, current Ah discharged and Ah charged) were collected once per second.

The data was used to identify parameters of the three cell models. Then, the models were used to predict terminal voltage for the tests. Figures 2–4 show a comparison between model predicted terminal voltage and actual measured terminal voltage for three representative tests: pulsed ±1C rates, pulsed ±2C rates and pulsed ±4C rates. In all plots, the red line is the true cell voltage and the blue line is the model's prediction.

In Figure 2 we see a comparison between the measured data and the output of the "combined model". Because this model has no filter states, relaxation effects are missing in the model prediction.

Figure 3 shows results from the "filter state" model. It does a much better job of capturing the relaxation dynamics, but is still noticeably flawed due to its nearly linear nature.

Figure 4 shows results from the "radial-basis-function model". The model output is nearly indistinguishable from the cell output. This model has learned the dynamics well. A 100-RBF network was used to show this result. The RMS estimation error was about 2mV, which is less than the quantization noise floor expected in our BMS implementation. Figure 5 shows a plot of model RMS estimation error versus the number of RBF kernels used. We see that this method allows arbitrary precision by increasing the number of RBFs until the desired accuracy goal is met.
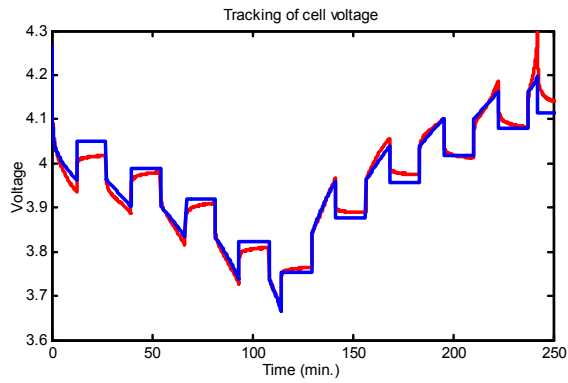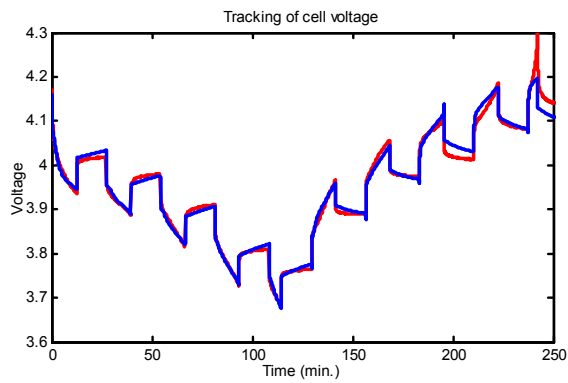
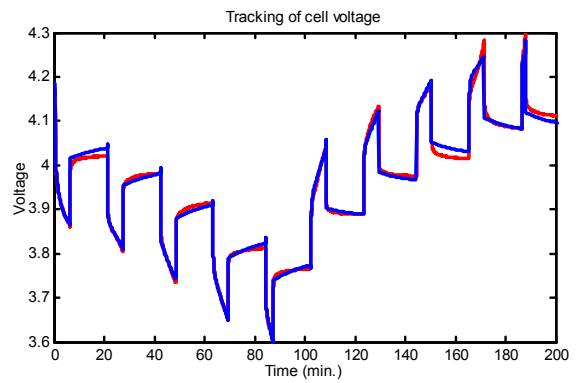Pulsed current at ±1C rates.
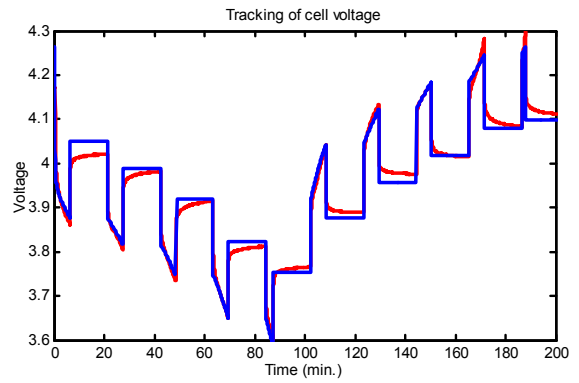
Pulsed current at ±2C rates.
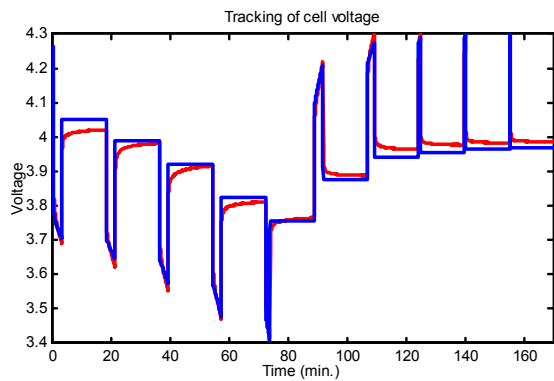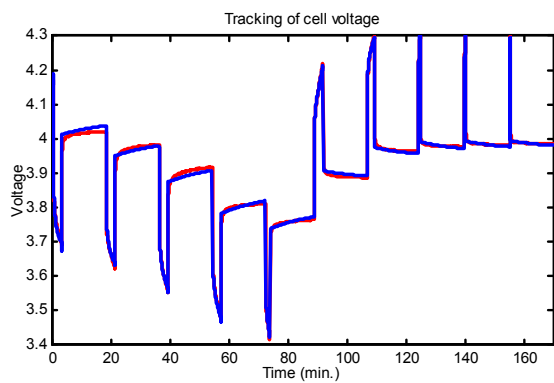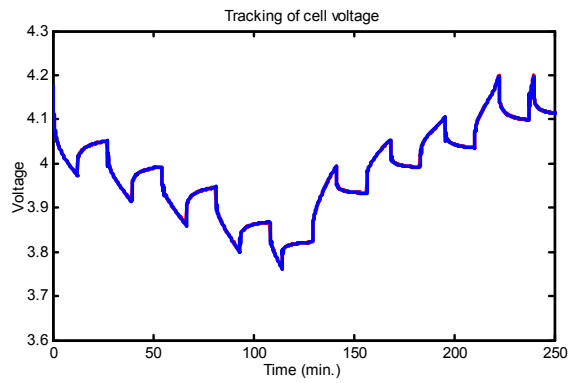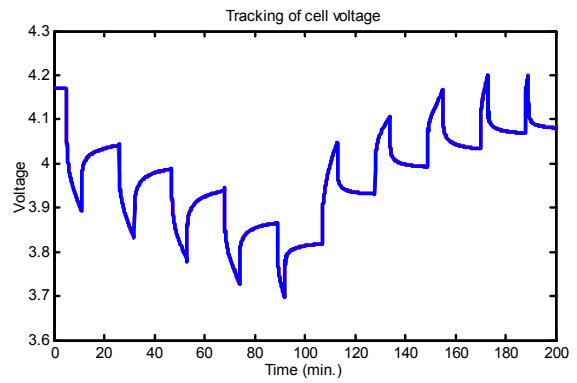

Pulsed current at ±4C rates.

Figure 2: Cell voltage tracking using the single-state model. Red line is true cell voltage; blue line is voltage predicted by cell model. Cell tests were pulsed current at ±1C, ±2C and ±4C rates, punctuated with rest periods.

Pulsed current at ±1C rates.

Pulsed current at ±2C rates.
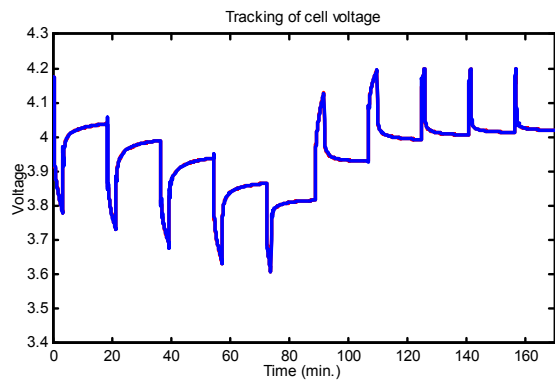

Pulsed current at ±4C rates.

Figure 3: Cell voltage tracking using the filter-state model. Red line is true cell voltage; blue line is voltage predicted by cell model. Cell tests were pulsed current at ±1C, ±2C and ±4C rates, punctuated with rest periods.

Pulsed current at ±1C rates.

Pulsed current at ±2C rates.

Pulsed current at ±4C rates.

Figure 4: Cell voltage tracking using the radial-basis-function network model. Red line is true cell voltage; blue line is voltage predicted by cell model. Cell tests were pulsed current at ±1C, ±2C and ±4C rates, punctuated with rest periods.
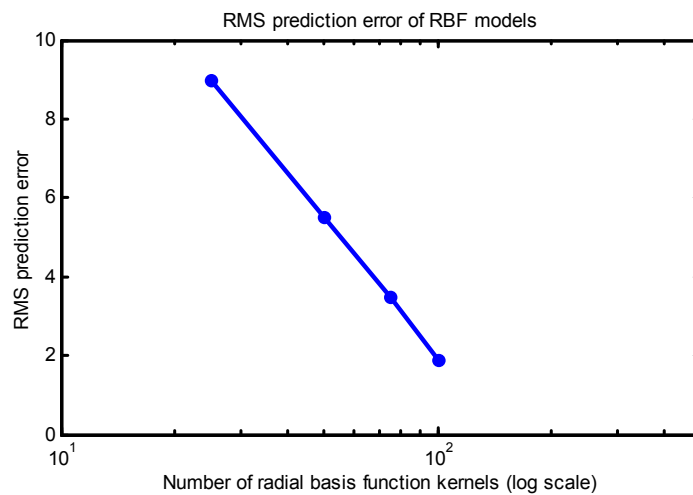

Figure 5: RMS prediction/modeling error using RBF networks with different numbers of basis functions (kernels).

Finally, Figure 6 shows results of a much more difficult modeling problem. Rather than simple pulsed charge/discharge cycles, it shows cell test results following a UDDS drive cycle, repeated a number of times over the SOC range of 0 to 1. An RBF network of the same size was used to identify this signal.

Note that space does not permit lengthy discussion of model temperature dependence. Preliminary work indicates that temperature may be included as another input to the RBF input vector for accurate modeling over the required temperature range.
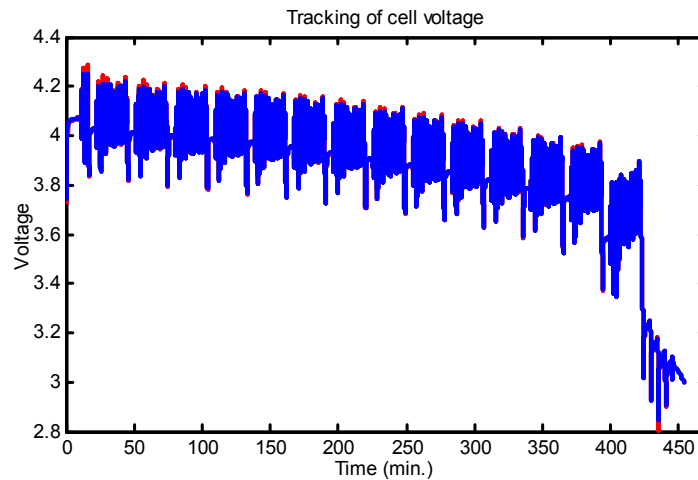

Figure 6: Tracking cell voltage in a very dynamic HEV test using the RBF model with 100 basis kernels.

5. Conclusions

This paper has proposed three mathematical state-space structures for the purpose of modeling LiPB HEV cell dynamics for the eventual purpose of SOC estimation via Kalman filtering. The single-state model is very simple, but performs the poorest. Adding filter states to the model aids performance, at some cost in complexity. The final structure, based on radial-basis-function networks, allows scalable complexity to model the dynamics as well as desired. It performed best of all. In addition, the companion paper [1] on SOC estimation shows that "the better the model, the better the SOC estimation". For this reason, the RBF model appears the best of those tested.

6. References

[1]   G. Plett, *Kalman-Filter SOC Estimation for LiPB HEV Cells*, Proceedings of the 19th International Battery, Hybrid and Fuel Cell Electric Vehicle Symposium & Exhibition (EVS19), 19–23 October 2002, Busan, Korea.

[2]   S. Piller, M. Perrin and A. Jossen, *Methods for state-of-charge determination and their applications*, Journal of Power Sources, vol. 96 (2001), pp. 113–120.

[3]   W. Gu and C. Wang, *Thermal-electrochemical modeling of battery systems*, Journal of the Electro-chemical Society, vol. 147, No. 8, (2000), pp. 2910–22.

[4]   K. Takano, K. Nozaki, Y. Saito, A. Negishi, K. Kato and Y. Yamaguchi, *Simulation study of electrical dynamic characteristics of lithium-ion battery*, Journal of Power Sources, vol. 90, no. 2, 2000, pp. 214–223.

[5]   E. Barsoukov, J. Kim, C. Yoon and H. Lee, *Universal battery parameterization to yield a non-linear equivalent circuit valid for battery simulation at arbitrary load,* Journal of Power Sources, vol. 83, no. 1–2, 1999, pp. 61–70.

[6]   S. Rodrigues, N. Munichandraiah and A. Shukla, *A review of state-of-charge indication of batteries by means of a.c. impedance measurements*, Journal of Power Sources, vol. 87, no. 1–2, 2000, pp. 12–20.

[7]   A. Salkind, C. Fennie, P. Singh, T. Atwater and D. Reisner, *Determination of state-of-charge and state-of-health of batteries by fuzzy logic methodology*, Journal of Power Sources, vol. 80. no. 1–2, 1999, pp. 293–300.

[8]   P. Singh, J. Fennie, D. Reisner and A. Salkind, *Fuzzy logic-enhanced electrochemical impedance spectroscopy (FLEEIS) to determine battery state of charge,* Proceedings of the 15th Annual Battery Conference on Applications and Advances, 11–14 January 2000, pp. 199–2004, Long Beach, CA.

[9]   A. Kawamura and T. Yanagihara, *State of charge estimation of sealed lead-acid batteries used for electric vehicles,* Proceedings of the 29th Annual IEEE Power Electronics Specialists Conference, 17–22 May 1998, pp. 582–7, Fukuoka, Japan.

[10]   S. Bhatikar, R. Mahajan, K. Kipke and V. Johnson, *Neural network based battery modeling for hybrid electric vehicles,* Proceedings of the 2000 Future Car Congress, 2–6 April 2000, (Paper No. 2000–01–1564), Arlington, VA.

[11]   H. Chan and D. Sutanto, *A new battery model for use with battery energy storage systems and electric vehicle power systems,* Proceedings of the 2000 IEEE Power Engineering Society Winter Meeting, 23–27 January 2000, pp. 470–5, Singapore.

[12]   V. Johnson, A. Pesaran and T. Sack, *Temperature-dependent battery models for high-power lithium-ion batteries,* Proceedings of the 17th Electric Vehicle Symposium (EVS-17), 15–18 October 2000, Montreal, Canada.

[13]   R. Giglioli, P. Pelachi, M. Raugi and G. Zini, *A state of charge observer for lead-acid batteries, Energia Elettrica*, vol. 65, no. 1. 1988, pp. 27–33.

[14]   C. Barbier, H. Meyer, B. Nogarede and S. Bensaoud, *A battery state of charge indicator for electric vehicle*, Proceedings of the Institution of Mechanical Engineers. Automotive Electronics. International Conference, 17–19 May 1994, pp. 29–34, London, UK.

[15]   W. Steffens and P. Lürkens, *Ladezustandsschätzung von bleibatterien mit hilfe des Kalman-filters*, etzArchiv, vol. 8, no. 7, 1986, pp. 231–6. (In German. English title: *State of charge estimation of lead-acid batteries using a Kalman filtering technique*).

[16]   ThermoAnalytics Inc., *Battery modeling for HEV Simulation by ThermoAnalytics Inc*, web site at http://www.thermoanalytics.com/support/publications/batterymodelsdoc.html, accessed 28 May 2002.

[17]   S. Haykin (Ed.), *Kalman Filtering and Neural Networks*, (Wiley Inter-Science: New York), 2001.

7. Affiliation

Dr. Gregory L. Plett, *Assistant Professor,*
Dept. of Electrical and Computer Engineering, University of Colorado at Colorado Springs,
1420 Austin Bluffs Parkway, P.O. Box 7150, Colorado Springs, CO 80933–7150 USA
Tel: +1–719–262–3468, Fax: +1–719–262–3589, E-mail: glp@eas.uccs.edu,
URL: http://mocha-java.uccs.edu, *and consultant to*
Compact Power Inc., 1200 S. Synthes Ave., Monument, CO 80132 USA
Tel: +1–719–488–1600x134, Fax: +1–719–487–9485, E-mail: gplett@compactpower.com.
URL: http://www.compactpower.com/.